International Journal of Chemical, Materials and Biomolecular Sciences
ISSN: 2415-6620
Vol:14, No:5, 2020

Application of Synthetic Monomers Grafted Xanthan Gum for Rhodamine B Removal in Aqueous Solution

T. Moremedi, L. Katata-Seru, S. Sardar, A. Bandyopadhyay, E. Makhado, M. Joseph Hato

***Abstract*—**The rapid industrialisation and population growth have led to a steady fall in freshwater supplies worldwide. As a result, water systems are affected by modern methods upon use due to secondary contamination. The application of novel adsorbents derived from natural polymer holds a great promise in addressing challenges in water treatment. In this study, the UV irradiation technique was used to prepare acrylamide (AAm) monomer, and acrylic acid (AA) monomer grafted xanthan gum (XG) copolymer. Furthermore, the factors affecting rhodamine B (RhB) adsorption from aqueous media, such as pH, dosage, concentration, and time were also investigated. The FTIR results confirmed the formation of graft copolymer by the strong vibrational bands at 1709 cm^{-1} and 1612 cm^{-1} for AA and AAm, respectively. Additionally, more irregular, porous and wrinkled surface observed from SEM of XG-g-AAm/AA indicated copolymerization interaction of monomers. The optimum conditions for removing RhB dye with a maximum adsorption capacity of 313 mg/g at 25 ^{0}C from aqueous solution were pH approximately 5, initial dye concentration = 200 ppm, adsorbent dose = 30 mg. Also, the detailed investigation of the isothermal and adsorption kinetics of RhB from aqueous solution showed that the adsorption of the dye followed a Freundlich model (R^2 = 0.96333) and pseudo-second-order kinetics. The results further indicated that this absorbent based on XG had the universality to remove dye through the mechanism of chemical adsorption. The outstanding adsorption potential of the grafted copolymer could be used to remove cationic dyes from aqueous solution as a low-cost product.

***Keywords*—**Xanthan gum, adsorbents, rhodamine B, Freundlich model.

I. Introduction

CATIONIC dyes including methylene blue (MB) and RhB, are among the primary contaminants and are of most significant concern because of their persistence in aqueous solution, even at low concentrations [1]. Once the dye is consumed beyond the amount allowed, it can cause serious health problems such as skin irritation, nausea, cancer, mutation, etc. [2]. Consequently, proper and efficient treatment of contaminated textile effluents before discharge is an essential environmental concern.

The adsorption has become the most effective and promising solution for treatment of aqueous solution containing dye due to its properties such as low cost and no harmful byproducts [3]. Polymeric materials, especially polysaccharide-based copolymers as adsorbents, have provided new materials to remove pollutants from aqueous solutions [4]. Polysaccharides can be characterized as non-toxic and highly hydrophilic biopolymers consisting of several small units of saccharides bound by glycosidic bonds [5]. These biopolymers are produced and used for energy storage and structural support in animals or plants [6].

One of the widely used biopolymers, XG is an anionic polysaccharide attained from a bacterial coat of *Xanthomonas campestris* [7]. This polymer is soluble in both hot and cold water and has a high viscosity at very low concentrations [8]. XG structure consists of the main chain (1 → 4)-linked β-D-glucopyranose units equipped with side chains of trisaccharide composed of glucuronic acid residue and two residues of mannose. In the terminal β-D-mannopyranose residue is (1 → 4)-linked residue of β-D-glucuronic acid and that in turn is (1 → 2)-linked to the non-terminal residue of α-D-mannopyranose [9]. It has unique properties such as stable over alkaline and acidic environments, water-soluble, thermally stable, non-toxic and biodegradable. Nevertheless, because of its water solubility, it cannot be used alone as an adsorbent [10]. Different ways have been proposed to overcome these shortcomings, including combination with other polymers, copolymerization, and surface grafting.

One of the best ways to use polysaccharides for different purposes is to copolymerize synthetic polymers onto a polysaccharide backbone. [11]. Acrylics occupy an essential position among synthetic polymers [12]. The wide range of vinyl and other monomers available over the past few decades suggests that grafting is a powerful method of producing substantial modification of polysaccharide properties, thereby increasing its range of use [13]. It has also been shown that poly(AA) and poly(AAm) graft copolymers with various biopolymers can be effective adsorbents for removing contaminants such as heavy metal ions and dyes. For example, Xu et al. reported vinyl modified mesoporous poly(AA)/SiO_2 composite for malachite green sorption, which showed a sorption capacity of 220.49 mg/g [14]. In another study, the graft copolymer of AAm-co-AA onto cellulose is used as an adsorbent to eliminate toxic inorganic metal ions (lead, zinc and copper) from aqueous solution. This adsorbent presented high adsorption capacities of 209 mg/g, 55.04 mg/g and 61.84 mg/g, respectively. [15].

Given the above information, the current study, therefore, emphasizes the analysis of AAm and AA graft copolymer analyzed by X-ray diffraction (XRD), thermogravimetric analysis (TGA), scanning electron microscope (SEM), among others. In addition, the effect of various parameters such as pH, dosage, time and concentration on RhB and MB cationic dyes adsorption is also investigated.

Lebogang Maureen Katata-Seru is with the North West University, South Africa (e-mail: Lebo.Seru@nwu.ac.za).

II. Technical Approach

A. Materials

Benzophenone (BP) was bought from Merck, India. Then, sodium lauryl sulphate (SLS) was obtained from Loba Chemie Pvt Mumbai, India [16]. Sigma Aldrich Chemical Company, USA, supplied AAm, AA, XG, RhB and MB. Ethanol is used as a solvent. RhB and MB (1000 ppm and 200 ppm respectively) stock solutions were prepared by dissolving a 1 g of dye in the 1000 mL of deionised water and further diluted for batch adsorption experiments. All experiments were performed with deionised water.

B. Synthesis of XG Grafted with AAm: AA (XG-g-AAm/AA)

The synthesis of XG-g-AAm/AA copolymer varying AAm: AA mass ratio was done using a slight modification method reported by [16]. Several SLS surfactant and BP photo-initiator amounts have been used. Through adding a minimum volume of the ethanol-water mixture, thick XG slurry was prepared for the preparation of the copolymer. The paste was taken in a petri dish and then added two monomers of AAm and AA. Added SLS to the mixture, BP was eventually blended with it and then irradiated for 30 minutes under UV ray. The mass was allowed to cool down and then washed with acetone to eliminate all unreacted BP. Acetone was decanted to remove the residue and then dried in a vacuum oven for 24 h at 50 °C until a constant weight was obtained [16].

C. Instrumentation

FTIR Analysis

The monomer-XG linkage was recorded by a Perkin Elmer 100 spectrometer, USA, in between the range 400 - 4000 cm^{-1}, with a resolution of 4 cm^{-1}. The uptake of MB and RhB after adsorption process was also analysed The XG and XG-g-AAm/AA spectra were also reported for comparison purposes.

XRD Analysis

The crystallographic structure and chemical composition of the grafted copolymer was done by XRD (Philips PW 1830, CuKα radiation, λ = 1.5406 A).

TGA Analysis

TGA determined the weight loss as a function of the temperature of raw polysaccharide and AAm/AA grafted XG copolymer by using Perkin Elmer STA 6000 instrument linked to a PolyScience digital temperature controller under N2 gas purged at a flow rate of 20 mL/min.

SEM Analysis

XG and grafted copolymer were analyzed with SEM for morphological studies using FE-SEM (Auriga Cobra focused-ion beam). A small amount of the samples was prepared by coating with gold before microscopy and images were collected using a JEOL-JSM 7500F (USA) microscope.

Zeta Potential

The surface charge of the copolymer was determined by dynamic light scattering using Malvern Zetasizer Nano-series (Malvern Instruments, United Kingdom). A nylon 0.45 µL pore size syringe filter was used to filter graft copolymer to eliminate potential dust particles prior to analysis. All experiments were carried out in triplicate.

D. Removal of MB and RhB Dye

The experiments were conducted to investigate the adsorption behaviour of the copolymer prepared in this study against the MB and RhB dyes. The effect of pH (1-10), the effect of dosage (10-50 mg), contact time (10-90 min), temperature (298.15-318.15 K), concentration (100-500 ppm) on the adsorption behaviour of XG-g AAm/AA were studied and compared to literature. The adsorption procedure follows as: An amount of 30 mg of XG-g-AAm/AA adsorbent was combined with 30 mL of RhB and MB dye solutions respectively, at a shaking speed of 200 rpm for 60 min. Afterwards, the samples were filtered using a syringe filter of 0.45 µm and the concentration of each dye were measured [16] by using UV-Vis spectrometer (Perkin Elmer Lambda model) at a wavelength of 664 nm (MB) and 553.70 nm (RhB). The adsorption capacity was then calculated as (1):

$$q_e = \frac{C_0 - C_e}{m} \times V \quad (1)$$

where q_e is the adsorption capacity per unit of adsorbent (mg/g), C_0 and C_e are the initial and final dye concentrations (mg/L), m is the adsorbent mass (mg), and v is the dye solution volume (L).

E. Adsorption Kinetics

Kinetic adsorption experiments were executed by mixing 30 mg of adsorbent with 60 mL of 200 mg/L of RhB and MB solutions, independently, at a constant speed (200 rpm) at different temperatures. In this study, four kinetics models were investigated, i.e. Lagergren's the pseudo-first-order (2) [17], pseudo-second-order (3) [18], Elovich (4) and intraparticle diffusion (5) [19].

$$\ln(q_e - q_t) = \ln q_e - K_1 t \quad (2)$$

$$\frac{t}{q_1} = \frac{1}{K_2 q^2_e} + \frac{1}{q_e} t \quad (3)$$

$$q_t = \frac{1}{\beta} \ln(\alpha\beta) + \frac{1}{\beta} \ln(t) \quad (4)$$

$$q_t = k_i t^{0.5} + C_i \quad (5)$$

whereas, k_1 and k_2 are the rate constants for pseudo-first and pseudo-second-order models respectively. The parameter β is associated with the extent of surface coverage, and activation energy for chemisorption (g/mg) and α is the initial sorption (mg/g/min).

F. Adsorption Isothermal Study

In order to check the isothermal sorption behaviour of the grafted copolymer on MB and RhB dyes (298.15-318.15 K), the sample with a weight of 10 mg was tested. The Temkin model (6) [20] Langmuir model (7) [17] and the Freundlich

model (8) [21] were used to fit the adsorption of cationic dyes data.

$$q_e = \frac{RT}{b_T} In\ K_T C_e \quad (6)$$

$$\frac{C_e}{q_e} = \frac{1}{q_m b} + \frac{1}{q_m} C_e \quad (7)$$

$$In\ q_e = InK_f + \frac{1}{n} InC_e \quad (8)$$

K_T (L/g) is the Temkin constant, R (8.314 J/mol K) the ideal gas constant, T is the absolute temperature (T), and b_T is the constant related to the heat of adsorption (J/mol). C_e is dye concentration at equilibrium (mg/L), q_e is the adsorbed dye quantity (mg/g) at equilibrium, K_f is Freundlich constant, n is the magnitude of the exponent.

G. Results and Discussion

Synthesis Mechanism of XG-g-AAm/AA

The UV irradiation technique was carried out to prepare XG-g-AAm/AA, BP as an initiator. The suggested mechanism of graft copolymerization can be observed in Fig. 1. The free radical site on XG created by an initiator radical through the abstraction of an H atom from the OH group. Initially, the initiator produces OH radicals, which subsequently generate active sites on XG and AA molecules, initiating the grafting reaction. The radical polymer sites facilitate the grafting of two vinyl monomers added to the reaction mixture copolymerization and result in the formation of the grafted copolymer.

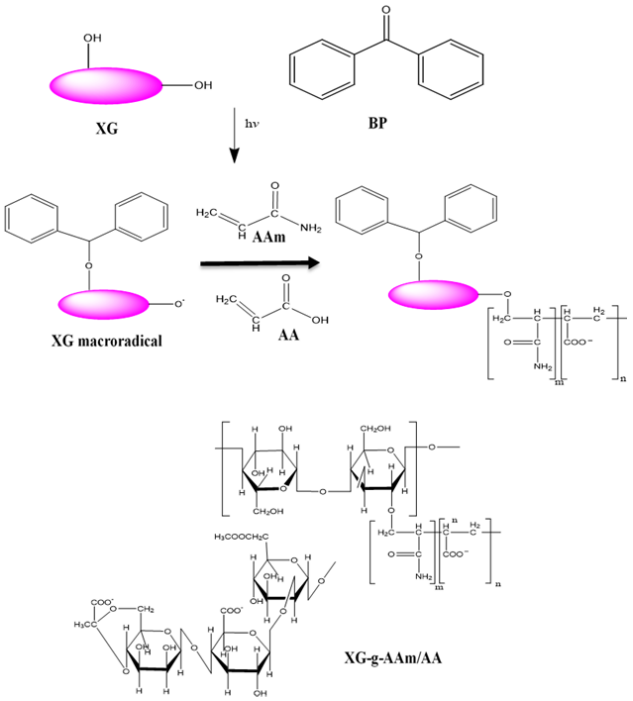

Fig. 1 A possible mechanism for the copolymerization of poly (AA-co -AAm) on XG

H. Characterization of Pure XG and Grafted Copolymer

FTIR Analysis

The structural changes of XG and XG grafted AAm and AA were elucidated using FTIR spectroscopy. XG alone is rich in carboxylic, hydroxyl and acetyl functional [22]. In the XG spectrum (Fig. 2 (a)), a broad peak appearing at 3263 cm^{-1} shows the stretching absorption vibration of O - H group, while at 2915 cm^{-1} represent the C – H stretching vibrations [23]. The two peaks at 1712 $cm^{-1}$and 1653 cm^{-1} are assigned to stretching vibration of carbonyl (C – O) of the acetyl group and asymmetrical stretching of C – O group of pyruvate group respectively [24]. Moreover, the absorption peaks at 1416 cm^{-1} and 1019 cm^{-1} due to the symmetrical stretching of –CCO- group of glucuronic acid and C – O – C of the ether group, respectively were revealed [25].

The formation of a grafted copolymer of XG-g-AAm/AA can be recognised from the peaks of 1402 cm^{-1} (C = O symmetric stretching) and 1593 cm^{-1} (C = O asymmetric stretching), which relates to carboxylate anion of AA [26]. The spectrum also exhibited a characteristic band at 3263 cm^{-1} which was due to overlap of N – H amide stretching [27]. The grafting of AA and AAm on to XG backbone was verified by the strong vibrational bands at 1709 cm^{-1} and 1612 cm^{-1} respectively [15]. FTIR spectra of MB loaded XG-g-AAm/AA, and RhB loaded XG-g-AAm/AA are shown, Fig. 2 (b). The FTIR results illustrated characteristic peak shifts indicating interactions between the dye and the adsorbent. The peak of 2895 cm^{-1} (C H stretching) showing no shift also suggests that adsorption occurs through electrostatic interaction as well as H-bonding between the dyes (MB and RhB) and the XG-g-AAm/AA [28].

TGA

The thermal stability of the synthesized samples was evaluated from 0-700 ^{0}C (Fig. 3 (a)). The interaction of the polymer and the monomers affected the thermal stability of the XG. The first weight loss of 11%, at 25-100 ^{0}C for XG and grafted copolymer respectively, was due to the loss of adsorbed water. The weight loss increases with temperature until 310 ^{0}C and thereafter decreases. About 40% of weight loss occurred between 150 and 310 ^{0}C. Finally, the total mass loss of about 56% degraded at 350 ^{0}C. The degradation results of XG-g-AAm/AA exhibited second degrading step, which occurred from 200 ^{0}C-410 ^{0}C with weight loss of 45% and final degradation occurred at 500 ^{0}C. The results indicated that the introduction of AA and AAm into XG polymer enhanced the thermal stability of the graft copolymer (25 ^{0}C to 460 ^{0}C)

XRD

The XRD depicted the amorphous nature of unmodified XG with a wide diffraction peak at 2θ = 20.1^0 (Fig. 3 (b)) compared to the spectra of XG-g-AAm/AA. On grafting of XG, the intensity increased with an additional characteristic peak of AA and AAm overlapping at 2θ = 43^0, which confirms the grafting of the copolymer. The overall results show that that grafting leads to disruption in the original amorphous structure of XG [29].

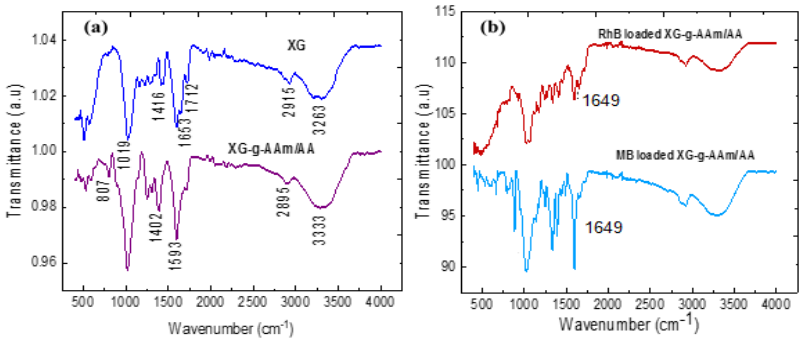

Fig. 2 FTIR spectra of (a) XG and XG-g-AAm/AA and RhB and MB dye loaded XG-g-AAm/AA

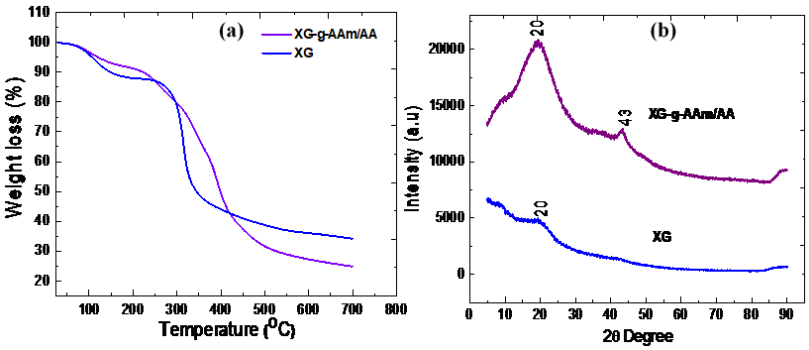

Fig. 3 TGA (a) and XRD (b) of XG, XG-g-AAm/AA copolymer

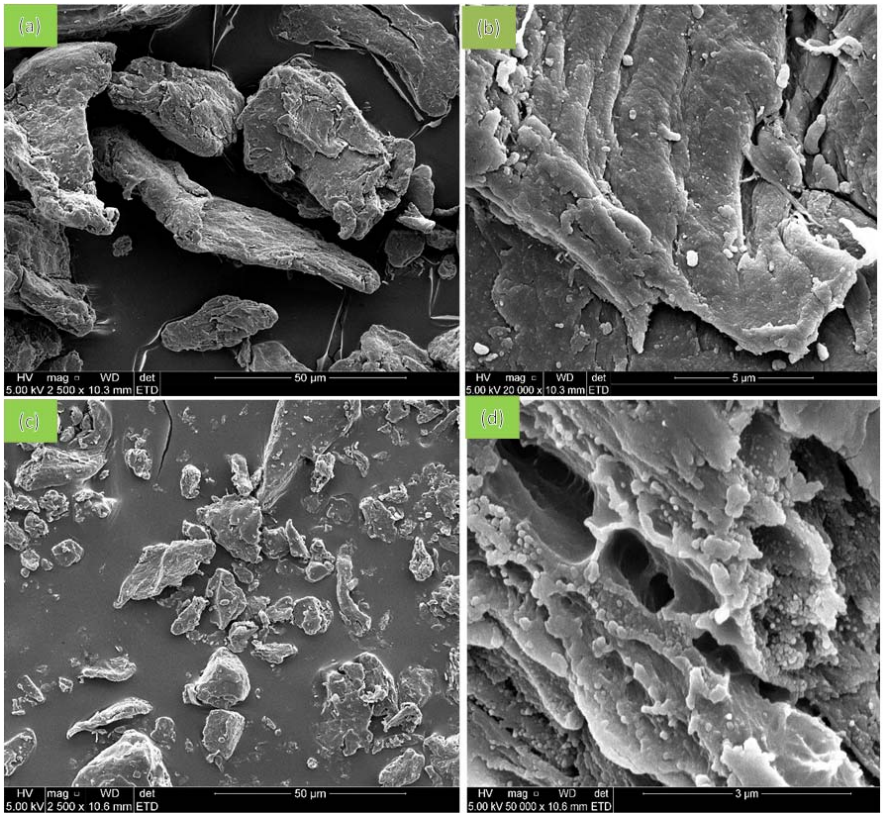

Fig. 4 SEM micrographs of (a), (b) XG and (c), (d) XG-g-AAm/AA

SEM Analysis

The morphological analysis of modified XG exhibited significant changes as compared to XG (Fig. 4) as observed in Figs. 4 (c), (d). The SEM images indicated that grafting of AAm-co-AA slightly changed from the rough flatted surface of XG (Figs. 4 (a), (b)) to more irregular shaped morphology. The copolymerization of monomers caused the porous and wrinkled morphology on the graft copolymer, which will improve the rate of adsorption and allow the diffusion of pollutants around the adsorption sites.

Adsorption Studies

Surface Charge Analysis

The surface charge for synthesized copolymer was characterized with the aid of zeta potential parameter. Fig. 5 (a) shows the zeta potential curve for the graft copolymer at various pHs. The results demonstrated that the zeta potential of XG-g-AAm/AA depended on the solution pH and had a negative charge for all pH values with the highest ζ-potential value of -54 mV. These observations can be explained by dissociating the hydroxyl groups that give the surface of the XG-g-AAm/AA the negative charge. This finding may have been due to −COOH group deprotonation with increased pH [30]. The negatively charged values obtained are therefore favourable for attraction between active sites and positive charges of the dyes, resulting in electrostatic attraction.

The Effect of pH on Dyes

Fig. 5 (b) shows a pH effect on the removal of MB and RhB. As observed, it is clear that from pH 1 to 3 the adsorption capacity of the cationic dyes on XG-g-AAm/AA adsorbent increased, and as the pH surpassed the value of 3, adsorption of RhB dye decreased continuously. The decrease is due to the ionisation of the carboxylic groups on the RhB that improves as the pH values increase. Consequently, the electrostatic repulsion between the adsorbate and adsorbent increases accordingly, because of less diffusion of RhB molecules into the copolymer. As for MB, the electrostatic attraction forces between N^+ and COO^- of the graft copolymer adsorbent is [31]. At solution pH < 4.0, the RhB molecules occur in cationic and monomeric forms and is able to easily enter in the pores of adsorbent but forms dimmers at solution pH > 4.0 because RhB molecule exists in the zwitterionic form [32]. From the overall results between the two dyes, XG-g-AAm/AA showed better adsorption capacity than RhB with q_e value of 255 mg/g to 160 mg/g respectively.

Adsorbent Dosage Effect

As can be seen in Fig. 5 (c), the adsorption capacity for both dyes decreases as the dosage is increased (10-50 mg). This is due to the increase of overlapping active adsorption sites. Also, the process of distributing dye molecules to the adsorption site takes time, leading to a decrease in adsorption [33]. In the case of MB, the maximum adsorption capacity (601 mg/g) was observed, whereas 342 mg/g for RhB was obtained when 10 mg of the adsorbent was utilized. This preference for MB dye may be typically from the steric hindrance due to the 2D planar structure of RhB molecules [34].

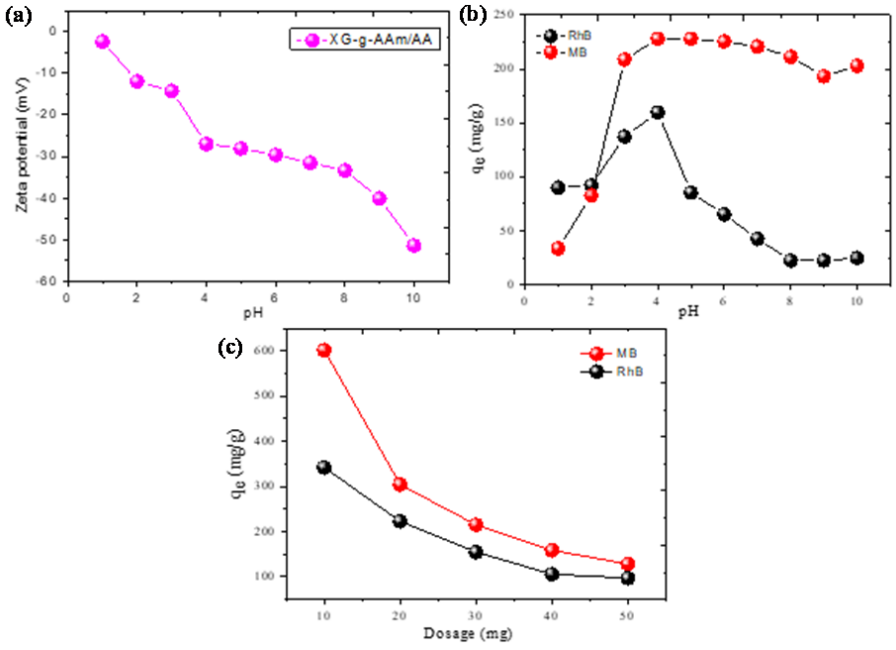

Fig. 5 Effect of (a) pH on zeta potential, (b) pH and (c) adsorbent dose on adsorption of RhB and MB from aqueous solution using XG-g-AAm/AA copolymer

Adsorption Isothermal Study

The adsorption isotherm is the connection between the amount of adsorbed dye and its concentrations in the equilibrium solution at a constant temperature. This analysis permits the maximum adsorption capacity of a given adsorbent to be determined, depending on the model applied, as shown in Figs. 6 and 7, respectively [35]. The value for correlation coefficient (R^2) for Langmuir plot (Table I) is closer to one, in the case of MB, meaning that the interaction between the adsorbent and the adsorbate depends on the homogeneity of the adsorbent (XG-g-AAm/AA) surface. In contrast to RhB, Freundlich model was found to be the best fitting curve of the adsorption process. This shows that the state that the surface of the adsorbent molecule is heterogeneous signifying multilayer adsorption. From the Temkin results also, it can be seen that this model is applicable for RhB adsorption. It can, therefore, be concluded that the surface of the adsorbent consists of multi-layered morphology.

TABLE I
ISOTHERMAL PARAMETERS OF XG-G-AAM/AA ADSORBENT FOR ADSORPTION OF DYES

Models	298.18 K		318.15 K		308.15 K	
	MB	RhB	MB	RhB	MB	RhB
Langmuir						
Qm	385.15	4437.74	735.26	3904.88	1209.50	1715.44
b	-0.094	0.0007	0.125	0.0007	0.014	0.0018
R^2	0.92255	-0.07005	0.9703	-0.11425	0.94919	-0.08192
Freundlich						
R^2	0.0645	0.92455	0.808	0.95097	0.9147	0.77669
n	13.33	1.07192	3.59842	1.10954	1.75839	1.40136
Temkin						
R^2	-0.27997	0.87075	0.64385	0.7754	0.92225	0.54545
b_T	89.15	7.59	19.12	8.41	9.20	10.82
B	27.79	326.59	133.99	304.69	287.51	244.45

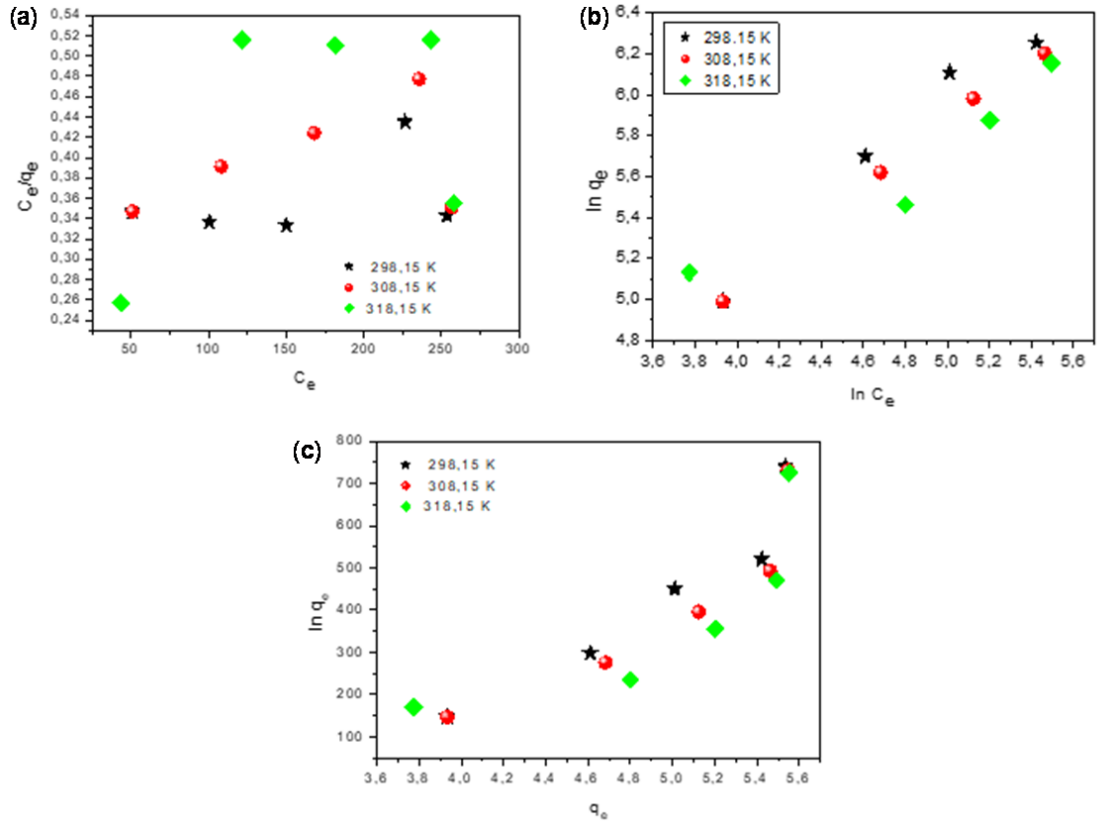

Fig. 6 Adsorption isotherm plots for RhB onto XG-g-AAm/AA, (a) Langmuir isotherm, (b) Freundlich model, and (c) Temkin model

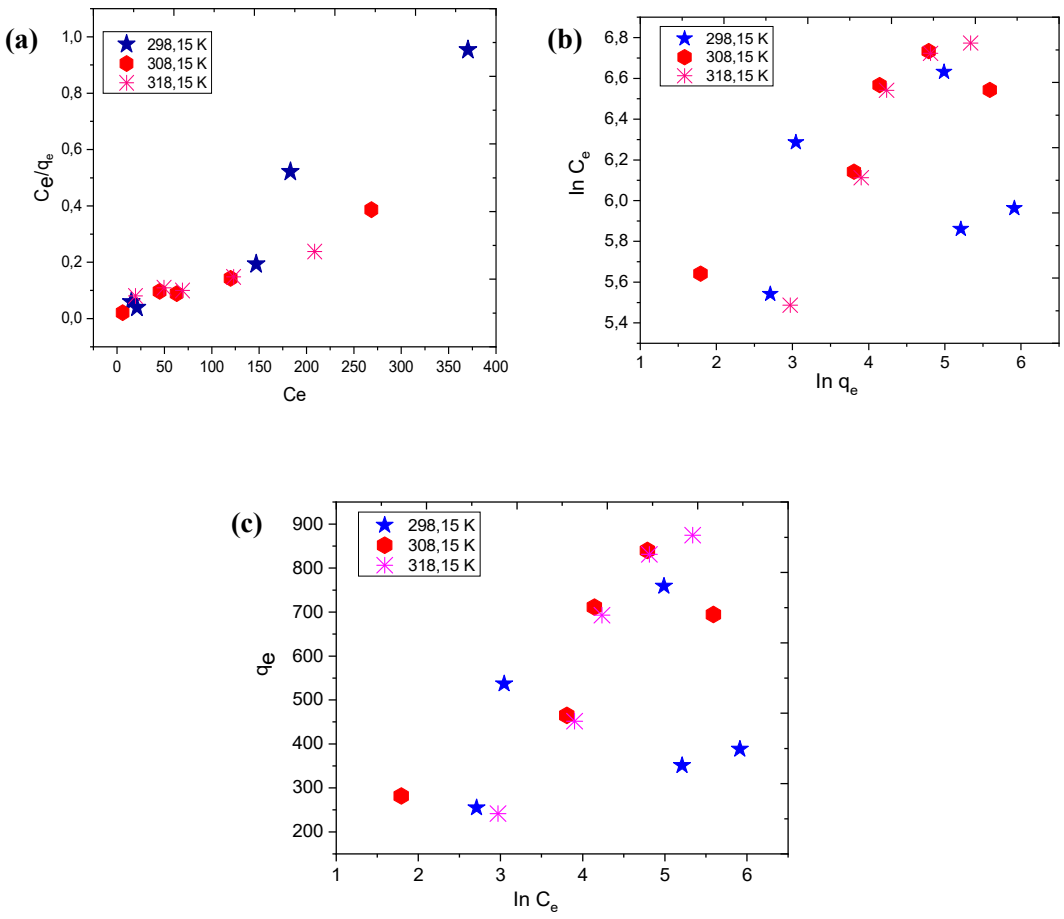

Fig. 7 Adsorption isotherm plots for MB onto XG-g-AAm/AA, (a) Langmuir isotherm, (b) Freundlich model, and (c) Temkin model

TABLE II
THE KINETIC MODELS FOR THE ADSORPTION OF MB AND RHB ON XG-G-AAM/AA

Models	298.18 K		318.15 K		308.15 K	
	MB	RhB	MB	RhB	MB	RhB
Pseudo first order						
q_e (mg/g)	-98.81	-34.36	-20.06	-42.64	-41.72	-72.09
K_1 (L/g)	0.23\31	0.0670	0.0115	0.0540	0.0552	0.0319
R^2	0.12582	0.51885	0.56624	0.17251	0.73282	0.25278
Pseudo second order						
R^2	0.9996	0.99803	0.99253	0.99571	0.99771	0.98975
q_e (mg/g)	512.82	258.39	296.73	354.61	448.43	312.5
K_2 (mg/g min)	0.00372	0.00279	0.0014	0.00169	0.00068	0.00101
Elovich						
R^2	0.3272	0.4076	0.50738	0.02672	0.81897	0.05234
B (g/mg)	0.09809	0.12378	0.06501	0.09344	0.0218	0.0604
Intraparticle diffusion						
R^2	0.27227	0.45408	0.521	0.076	0.72916	0.1085
C (mg/g)	485.325	228.425	240.974	309.941	304.624	243.297
K_{id} (mg/g $min^{1/2}$)	3.574	3.10494	5.75273	4.37384	16.2043	6.77903

Adsorption Kinetic Studies

The contact time of the liquid and solid as well as the diffusion process influence the rate of dye uptake. Hence, Figs. 8 and 9 depict the adsorption kinetics curve fittings in understanding the adsorption mechanism with the pseudo-first-order, pseudo-second-order, Elovich and intraparticle diffusion. Summary of the corresponding parameters calculated from the above four models is seen in Table II. The pseudo-second-order offered high R^2 values for both MB (0.9996 – 0.9977) and RhB (0.98957 - 0.99803), compared of intraparticle diffusion, Elovich and pseudo-first-order. This implies that MB showed better interaction with the adsorbate than RhB. In addition, it verifies that, in comparison to physisorption, the adsorption rate occurred by chemisorption.

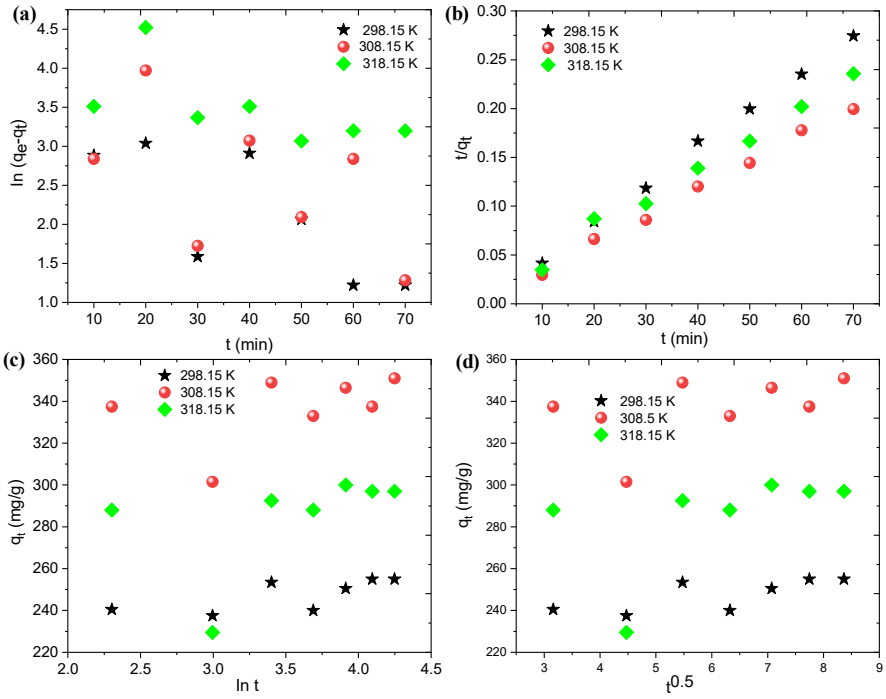

Fig. 8 Adsorption kinetic plots for RhB onto XG-g-AAm/AA (a) pseudo-first-order, (b) pseudo-second-order, (c) Elovich model and (d) interparticle diffusion model

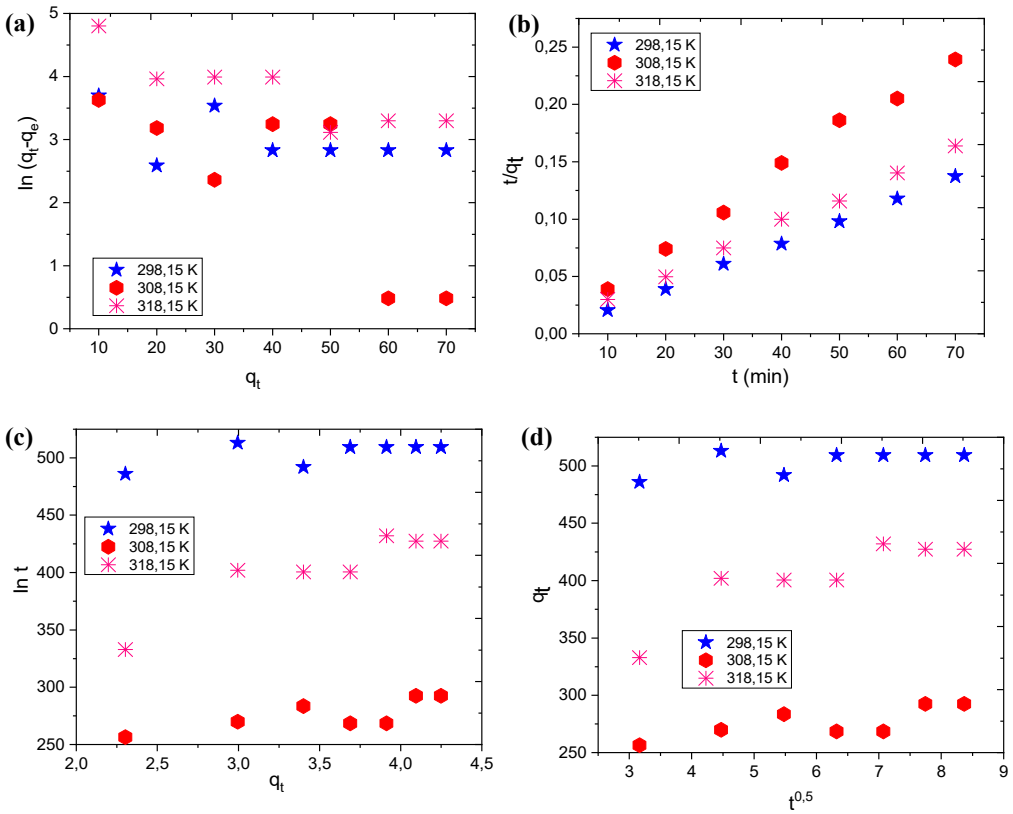

Fig. 9 Adsorption kinetic plots for MB onto XG-g-AAm/AA (a) pseudo-first-order, (b) pseudo-second-order, (c) Elovich model and (d) interparticle diffusion model

III. Conclusion

The synthesis of polymer (XG) and its graft copolymer was prepared using UV irradiation technique. Best conditions for a higher percentage of dye adsorption using XG-g-poly (AA-co-AAm) polymer adsorbent: pH of 5 (RhB) and 6 (MB) adsorbent solution; 10 mg adsorbent. The studies of adsorption isotherm found that the Langmuir isotherm model best suited and explained the equilibrium data for MB while the Freundlich model fitted data were for RhB. Furthermore, kinetic studies exhibited that the adsorption of both RhB and MB on the copolymer is a chemisorption process. It can be inferred from this analysis that the XG-g-AAm/AA can be used as an adsorbent to adsorb RhB and MB dyes from dye contaminated water.

Acknowledgment

The financial assistance from North-West University (NWU), DST/NRF-Sasol foundation, Thuthuka program (117727) is greatly acknowledged. The authors also acknowledge the technical support by Chemistry department (University of Calcutta), Faculty of Natural and Agricultural Sciences, NWU, Chemistry department (University of Limpopo), Council for Scientific and Industrial Research, South Africa.

References

[1] M. T. Uddin, M. A. Rahman, M. Rukanuzzaman, M. A. Islam, Applied Water Science 2017, 7, 2831-2842.
[2] Y. Jiang, B. Liu, J. Xu, K. Pan, H. Hou, J. Hu, J. Yang, Carbohydrate polymers 2018, 182, 106-114.
[3] X. Zhao, L. Lv, B. Pan, W. Zhang, S. Zhang, Q. Zhang, Chemical engineering journal 2011, 170, 381-394.
[4] L. Dehabadi, L. D. Wilson, Carbohydrate polymers 2014, 113, 471-479.
[5] M. R. Guilherme, F. A. Aouada, A. R. Fajardo, A. F. Martins, A. T. Paulino, M. F. Davi, A. F. Rubira, E. C. Muniz, European Polymer Journal 2015, 72, 365-385.
[6] Y. Zheng, J. Monty, R. J. Linhardt, Carbohydrate research 2015, 405, 23-32.
[7] D. F. Petri, Journal of Applied Polymer Science 2015, 132.
[8] B. d. M. Lopes, V. L. Lessa, B. M. Silva, L. G. La Cerda, J Food Nutr Res 2015, 54, 185-194.
[9] M. N. Hazirah, M. Isa, N. Sarbon, Food Packaging and Shelf Life 2016, 9, 55-63.
[10] M. H. A. Elella, M. W. Sabaa, E. A. ElHafeez, R. R. Mohamed, International journal of biological macromolecules 2019, 137, 1086-1101.
[11] G. Sharma, M. Naushad, D. Pathania, A. Mittal, G. El-Desoky, Desalination and Water Treatment 2015, 54, 3114-3121.
[12] M. Bhabhe, P. Galvankar, V. Desai, V. Athawale, Journal of applied polymer science 1995, 56, 485-494.
[13] R. C. Mundargi, S. A. Patil, T. M. Aminabhavi, Carbohydrate Polymers 2007, 69, 130-141.
[14] R. Xu, M. Jia, Y. Zhang, F. Li, Microporous and Mesoporous Materials 2012, 149, 111-118.
[15] A. Guleria, G. Kumari, E. C. Lima, Carbohydrate polymers 2020, 228, 115396.
[16] A. Pal, K. Majumder, A. Bandyopadhyay, Carbohydrate polymers 2016, 152, 41-50.
[17] S. K. Lagergren, Sven. Vetenskapsakad. Handingarl 1898, 24, 1-39.
[18] Y.-S. Ho, G. McKay, Process biochemistry 1999, 34, 451-465.
[19] W. J. Weber, J. C. Morris, Journal of the Sanitary Engineering Division 1963, 89, 31-60.
[20] M. Temkin, V. Pyzhev, 1940.
[21] H. Freundlich, Chem, 1906.
[22] L. Su, W. Ji, W. Lan, X. Dong, Carbohydrate Polymers 2003, 53, 497-499.
[23] S. Pal, S. Ghorai, C. Das, S. Samrat, A. Ghosh, A. B. Panda, Industrial & Engineering Chemistry Research 2012, 51, 15546-15556.
[24] E. D. Raczyńska, K. Duczmal, M. Darowska, vibrational Spectroscopy 2005, 39, 37-45.
[25] S. Thakur, S. Pandey, O. A. Arotiba, Carbohydrate polymers 2016, 153, 34-46.
[26] S. Kaur, R. Jindal, Materials Chemistry and Physics 2018, 220, 75-86.
[27] D. A. Bhagwat, V. R. Kolekar, S. J. Nadaf, P. B. Choudhari, H. N. More, S. G. Killedar, Carbohydrate Polymers 2020, 229, 115357.
[28] Y. Fang, A. Zhou, W. Yang, T. Araya, Y. Huang, P. Zhao, D. Johnson, J. Wang and Z.J. Ren, Scientific reports 2018., 8(1), 229.
[29] H.R. Badwaik, K. Sakure, A. Alexander, H. Dhongade. and D.K. Tripathi, International journal of biological macromolecules 2016, 85,.361-369.
[30] X. T. Le, S. L. Turgeon, Soft Matter 2013, 9, 3063-3073.
[31] Y. Tang, T. He, Y. Liu, B. Zhou, R. Yang, L. Zhu, Advances in Polymer Technology 2018, 37, 2568-2578.
[32] A. Thakur, H. Kaur, International Journal of Industrial Chemistry 2017, 8, 175-186.
[33] N. B. Shukla, G. Madras, Journal of Applied Polymer Science 2012, 124, 3892-3899.
[34] H. Mittal, V. Kumar, S. M. Alhassan, S. S. Ray, International journal of biological macromolecules 2018, 114, 283-294.
[35] D. L. Postai, C. A. Demarchi, F. Zanatta, D. C. C. Melo, C. A. Rodrigues, Alexandria Engineering Journal 2016, 55, 1713-1723.